



On automatic determination of quasicrystal orientations by indexing of detected reflections

Adam Morawiec

Acta Cryst. (2023). **A79**, 339–344



IUCr Journals

CRYSTALLOGRAPHY JOURNALS ONLINE

Author(s) of this article may load this reprint on their own web site or institutional repository and on not-for-profit repositories in their subject area provided that this cover page is retained and a permanent link is given from your posting to the final article on the IUCr website.

For further information see <https://journals.iucr.org/services/authorrights.html>



On automatic determination of quasicrystal orientations by indexing of detected reflections

Adam Morawiec*

Institute of Metallurgy and Materials Science, Polish Academy of Sciences, Reymonta 25, Krakow, 30-059, Poland.

*Correspondence e-mail: nmmorawi@cyf-kr.edu.pl

Received 7 February 2023

Accepted 25 April 2023

Edited by L. Palatinus, Czech Academy of Sciences, Czech Republic

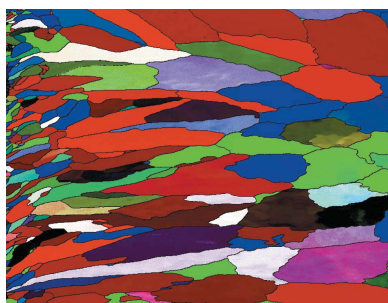
Keywords: quasicrystals; orientation mapping; diffraction; indexing; EBSD; microstructure.

Automatic crystal orientation determination and orientation mapping are important tools for research on polycrystalline materials. The most common methods of automatic orientation determination rely on detecting and indexing individual diffraction reflections, but these methods have not been used for orientation mapping of quasicrystalline materials. The paper describes the necessary changes to existing software designed for orientation determination of periodic crystals so that it can be applied to quasicrystals. The changes are implemented in one such program. The functioning of the modified program is illustrated by an example orientation map of an icosahedral polycrystal.

1. Introduction

The determination of orientations of crystallites, in particular for orientation mappings, is an important aspect of studies of polycrystals. However, data on the orientation statistics of quasicrystalline materials are scarce. At present, quasicrystals are not supported by the widely used fast commercial orientation mapping systems relying on the detection of individual reflections and conventional indexing, *i.e.* on assigning indices to the reflections. Therefore, electron backscatter diffraction (EBSD) orientation maps of quasicrystalline aggregates have been obtained by computer-aided manual indexing (Tanaka *et al.*, 2016), by matching experimental patterns to simulated patterns (Singh *et al.*, 2019) or to patterns obtained from a master reference pattern (Winkelmann *et al.*, 2020), and by automatic indexing using lattices of periodic approximants of quasicrystals (Cios *et al.*, 2020); see also Baker *et al.* (2017), Becker & Leineweber (2018), Leskovar *et al.* (2018) and Labib *et al.* (2019, 2020).

The question is, how difficult is the conventional indexing of quasicrystal diffraction patterns? The general idea is simple and well known: one needs to replace the lattice basis by a frame or overcomplete set of ‘basis’ vectors (Elser, 1985). In practice, however, it is deemed in some quarters that indexing quasicrystal diffraction patterns is complicated. The methods described by Tanaka *et al.* (2016), Singh *et al.* (2019), Winkelmann *et al.* (2020) and Cios *et al.* (2020) are ways around the problem of conventional indexing of such patterns. This paper demonstrates that the investment in adapting existing indexing software to solve quasicrystal diffraction patterns is relatively small. The necessary changes are described in detail and implemented in one of the indexing programs. The arguments are illustrated by an EBSD orientation map of an icosahedral polycrystalline material.



2. From periodic crystals to quasicrystals

2.1. Orientations of periodic crystals

It is worth recalling some basic facts about orientation determination by indexing of detected reflections for periodic crystals. Let \mathbf{s} denote a scattering vector normal to a reflecting crystal plane. In crystal diffraction, the scattering vector points to a node of the crystal reciprocal lattice, *i.e.* it has the form of the integer combination $\mathbf{s} = h\mathbf{a}^* + k\mathbf{b}^* + l\mathbf{c}^*$, where hkl are the reflection indices and \mathbf{a}^* , \mathbf{b}^* , \mathbf{c}^* are basis vectors of the reciprocal lattice. With the vectors \mathbf{a}^* , \mathbf{b}^* , \mathbf{c}^* renamed as \mathbf{a}^1 , \mathbf{a}^2 , \mathbf{a}^3 , and the indices hkl renamed as $l_1l_2l_3$, then using the summation convention the above expression takes the form

$$\mathbf{s} = l_i \mathbf{a}^i. \quad (1)$$

Besides having the basis vectors \mathbf{a}^i and the basis \mathbf{a}_i of the direct lattice, it is convenient to equip the crystal with a rigidly attached right-handed Cartesian system based on vectors $\mathbf{e}_i = \mathbf{e}^i$ in which the coordinates of \mathbf{s} are s_i , *i.e.* $\mathbf{s} = s_i \mathbf{e}^i$. Since the vectors \mathbf{e}_i , \mathbf{a}^i and \mathbf{a}_i are known *a priori*, so are their dot products. In particular, by definition, one has $\mathbf{a}_i \cdot \mathbf{a}^j = \delta_i^j$, where δ is the Kronecker delta. Knowing the indices $l_1l_2l_3$ (*i.e.* hkl) of the reflecting plane, one can get the Cartesian coordinates,

$$s_i = \mathbf{s} \cdot \mathbf{e}_i = l_j \mathbf{a}^j \cdot \mathbf{e}_i = l_j B_{ij}^j, \quad (2)$$

where $B_{ij}^j = \mathbf{a}^j \cdot \mathbf{e}_i$ is the i th Cartesian component of the j th basis vector of the reciprocal lattice.

Diffraction patterns are made up of traces of diffraction reflections. Based on the position of a trace, one computes the coordinates s_i^L of the scattering vector \mathbf{s} in the right-handed laboratory Cartesian coordinate system based on vectors \mathbf{e}_L^i , *i.e.* one has $\mathbf{s} = s_i^L \mathbf{e}_L^i$. The coordinates s_i and s_i^L are related by

$$s_i = \mathbf{s} \cdot \mathbf{e}_i = s_j^L \mathbf{e}_L^j \cdot \mathbf{e}_i = O_i^j s_j^L, \quad (3)$$

where $O_i^j = \mathbf{e}_L^j \cdot \mathbf{e}_i$ are entries of the special orthogonal matrix O representing the sought orientation of the crystal in the laboratory reference system.

In an experiment, a number of diffraction reflections are detected, so one has the coordinates s_i^L of vectors of a certain set, say G . On the other hand, there are numerous crystal planes which may lead to detectable reflections. Using the indices of potential high-intensity reflections, one obtains the coordinates s_i of vectors of another set, say H . The problem of orientation determination is to obtain the matrix O relating (as many as possible) vectors from G to some vectors from H . The problem can be seen as matching the largest possible subset of G to a subset of H . For descriptions of suitable algorithms, see *e.g.* Morawiec (2022) and references therein.

Details of how to calculate the coordinates of the vectors of the G set depend on the diffraction technique, but generally the method is simply based on the definition of the scattering vector: the vector is the difference between the wavevectors of the reflected beam and the incident beam.

As for the vectors of H , one usually starts with indices of a single representative of each detectable family of symmetrically equivalent reflections, and then the coordinates of the

scattering vectors corresponding to other reflections of the family are determined by using all symmetry operations for the crystal point symmetry: from the indices l_j of the representative, one obtains the coordinates $s_i = l_j B_{ij}^j$ of the corresponding scattering vector, and with the orthogonal matrix R representing a point symmetry in the basis \mathbf{e}_i , the coordinates of the equivalent vector are $R_i^j s_j$. Note, though, that care must be taken in cases where the vectors overlap with symmetry elements and the number of distinct vectors is smaller than the number of symmetry operations.

The integrity of the orientation determination procedure is confirmed by explicitly assigning indices to individual reflections. To this end, the list of vectors in H can be accompanied by a table with the indices of vectors on the list, but a more convenient approach is to calculate the indices directly from the s_i coordinates without creating any additional tables. The indices are $l_i = l_j \mathbf{a}^j \cdot \mathbf{a}_i = s_j \mathbf{e}^j \cdot \mathbf{a}_i = A_i^j s_j$, where $A_i^j = \mathbf{a}_i \cdot \mathbf{e}^j$ is the j th Cartesian component of the i th basis vector of the direct lattice. If the coordinates are inaccurate, such as those computed based on a symmetry operation or obtained from experimental s_i^L via equation (3), the indices are

$$l_i = \lfloor \mathbf{s} \cdot \mathbf{a}_i \rfloor = \lfloor A_i^j s_j \rfloor, \quad (4)$$

where $\lfloor x \rfloor$ denotes the integer nearest to real x . If the magnitude of \mathbf{s} is not known, as in the case of scattering vectors corresponding to EBSD bands, one needs to test all admissible magnitudes.

2.2. Orientations of quasicrystals

The question is how the case of a quasicrystal differs from that of a periodic crystal. As was already noted, the lattice basis \mathbf{a}^i ($i = 1, 2, 3$) must be replaced by a frame, *i.e.* an overcomplete set of vectors \mathbf{a}^μ , where $\mu = 1, 2, \dots, n \geq 3$ (Elser, 1985). Every scattering vector can be expressed as a linear integer combination of the vectors \mathbf{a}^μ . The expressions (1) and (2) need to be replaced by

$$\mathbf{s} = l_\mu \mathbf{a}^\mu \quad \text{and} \quad s_i = \mathbf{s} \cdot \mathbf{e}_i = l_\mu \mathbf{a}^\mu \cdot \mathbf{e}_i = l_\mu B_{i\mu}^\mu, \quad (5)$$

where l_μ are reflection indices and $B_{i\mu}^\mu = \mathbf{a}^\mu \cdot \mathbf{e}_i$.

The vectors \mathbf{a}^μ correspond to the basis \mathbf{a}^i of the reciprocal lattice, whereas, as a rule, the input of orientation determination systems dealing with periodic data contains the basis of the direct lattice. To stay within this convention, one needs to input the frame \mathbf{a}_μ dual to \mathbf{a}^μ . The set of vectors \mathbf{a}_μ can be viewed as one whose subsets span quasicrystal tilings in physical space, *i.e.* vectors pointing to the vertices of tiles can be expressed as linear integer combinations of the vectors \mathbf{a}_μ .

The Cartesian coordinates $B_{i\mu}^\mu$ of the vectors \mathbf{a}^μ are obtained from the input coordinates $A_{\mu i} = \mathbf{a}_\mu \cdot \mathbf{e}^i$ of the vectors \mathbf{a}_μ using the generalized (Moore–Penrose) inverse (Ben-Israel & Greville, 2003) of the transposed matrix A , *i.e.* $B = (A^T)^+$. Clearly, if $n = 3$, the vectors \mathbf{a}_μ are linearly independent, the matrix A is invertible and B is the regular inverse of A^T .

One also needs to recall that quasicrystals have the inflation/deflation property. Unlike the (Niggli-reduced) bases of a

periodic crystal lattice, frames characterizing quasicrystals and their diffraction patterns are not unique; they can be inflated or deflated (Elser, 1985). However, this is not an issue here because a specific frame \mathbf{a}_μ is selected, and one only needs to ensure that the indices l_μ are correct for the dual frame \mathbf{a}^μ .

In the case of icosahedral quasicrystals, it is convenient to use the frame of Bancel *et al.* (1985) with $n = 6$ and the vectors

$$\begin{aligned} \mathbf{a}^1 &= (\mathbf{e}^1 + \tau\mathbf{e}^2)/a & \mathbf{a}^2 &= (\mathbf{e}^1 - \tau\mathbf{e}^2)/a \\ \mathbf{a}^3 &= (\mathbf{e}^2 + \tau\mathbf{e}^3)/a & \mathbf{a}^4 &= (\mathbf{e}^2 - \tau\mathbf{e}^3)/a \\ \mathbf{a}^5 &= (\mathbf{e}^3 + \tau\mathbf{e}^1)/a & \mathbf{a}^6 &= (\mathbf{e}^3 - \tau\mathbf{e}^1)/a \end{aligned} \quad (6)$$

along fivefold symmetry axes; the vectors \mathbf{e}^i are along twofold axes, τ denotes the golden ratio and a is a structural parameter. The direct-space frame \mathbf{a}_μ dual to Bancel's frame \mathbf{a}^μ is given by $\mathbf{a}_\mu = \mathbf{a}^\mu/[2(\tau + 2)]$. For alternative frames, see Elser (1985), Katz & Duneau (1986) and Cahn *et al.* (1986).

Replacement of the lattice basis by a frame affects the generation of the theoretical scattering vectors of the set H . One complication is obtaining the indices of symmetrically equivalent reflections. Lists of equivalent indices for some quasicrystal symmetries are given by Morawiec (2022). Moreover, the indexing based on equation (4) cannot be easily generalized to quasicrystals. A procedure described in Section 13.5 of Morawiec (2022) generalizes the conventional $l_i = \mathbf{s} \cdot \mathbf{a}_i = A_i^j s_j$, but it relies on a distinction between rational and irrational numbers, and it is inapplicable to inaccurate data. An approach applicable to such data for icosahedral quasicrystals is given in the Appendix.

All other aspects of quasicrystal orientation determination remain the same as for periodic crystals. In particular, the method of calculating the measured scattering vectors of G is

the same for both periodic crystals and quasicrystals. As with periodic crystals, to obtain H it is generally assumed that representatives of the families of reflections that make up the diffraction patterns are known *a priori*. Finally, the method of matching the largest possible subset of G to a subset of H does not need to be changed.

2.3. Modifications to indexing software

The guidelines described in the previous section were used to modify *KiKoch2*, a program for orientation determination via indexing of diffraction patterns, which was originally developed for dealing with periodic crystals. For a description of the original program, see Morawiec (2020).

With n denoting the number of frame-spanning vectors, the main change to the program is that the modified version allows for n to be larger than 3. The default value of n (which is 3) can be changed in the input (Fig. 1). The other input data affected by this change are, first, the table A with the coordinates A_μ^i of vectors \mathbf{a}_μ of the direct-space frame, and second, the lists of indices l_μ of the representatives of families of reflecting planes in the frame \mathbf{a}^μ . With the dimension of the frame set to n , the table A consists of $n \times 3$ entries (instead of 3×3 entries for basis vectors), and the number of indices representing a family of reflectors is n (instead of 3).

The only significant internal modification to the program concerns the calculation of the (reciprocal-space) frame \mathbf{a}^μ from the input (direct-space) frame \mathbf{a}_μ . The subroutine for calculating the regular inverse of a matrix is replaced by code for numerical computation of the Moore–Penrose inverse.

<pre> _LatticeBasis 1.0000000 0.0000000 0.0000000 0.0000000 1.0000000 0.0000000 0.0000000 0.0000000 1.0000000 _NumberOfFamiliesOfReflectingPlanes 4 _FamiliesOfReflectingPlanes 1 1 1 0 0 2 0 2 2 1 1 3 _NumberOfSymmetryOperations 24 _SymmetryOperations 0.0000 0.0000 1.0000 0.00 1.0000 0.0000 0.0000 90.00</pre>	<pre> _NumberOfBasisVectors 6 _LatticeBasis 1.0000000 1.6180340 0.0000000 1.0000000 -1.6180340 0.0000000 0.0000000 1.0000000 1.6180340 0.0000000 1.0000000 -1.6180340 1.6180340 0.0000000 1.0000000 -1.6180340 0.0000000 1.0000000 _NumberOfFamiliesOfReflectingPlanes 2 _FamiliesOfReflectingPlanes 1 0 0 0 0 0 1 1 0 0 0 0 _NumberOfSymmetryOperations 60 _SymmetryOperations 0.0000 0.0000 1.0000 0.00 1.0000 0.0000 0.0000 180.00</pre>
--	---

Figure 1

Parts of headers of input files for processing typical EBSD data for (left-hand column) face-centred cubic metals and (right-hand column) icosahedral quasicrystals. The keywords used in the original version of *KiKoch2* have been left unchanged so that the modified program can process old data. The main difference is that the number of frame vectors defaults to 3 in the left column, and it is set at 6 in the right column. Consequently, the number of indices specifying families of reflectors is 3 in the left column and 6 in the right column. Clearly, the two cases also differ in the number and type of point symmetry operations.

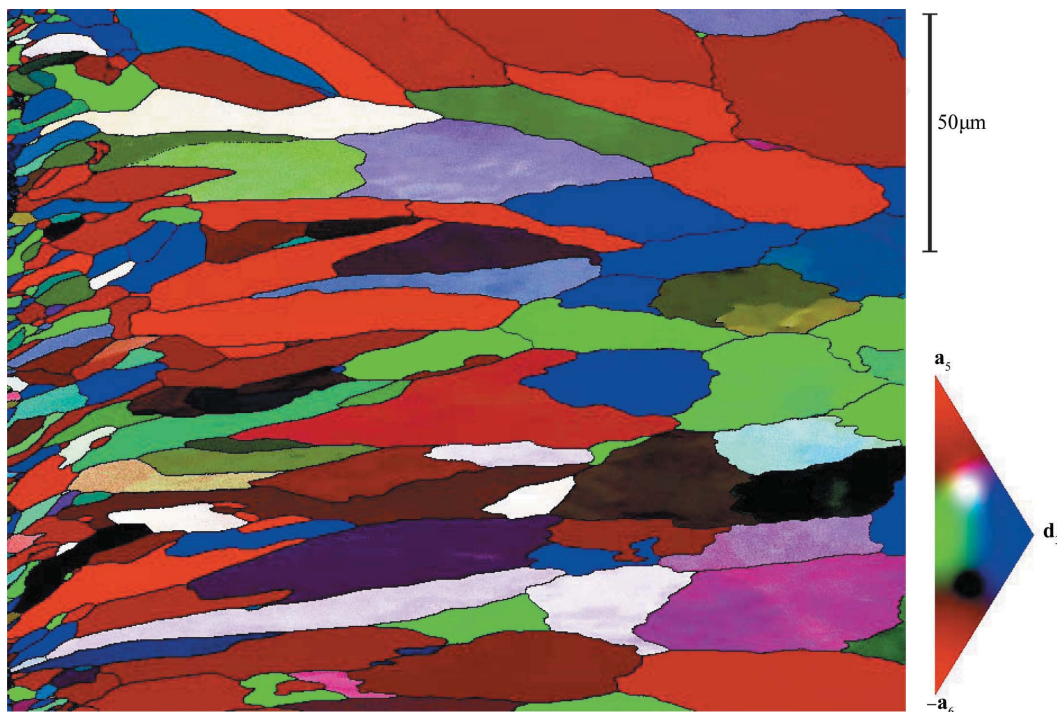


Figure 2
 An orientation map of the icosahedral quasicrystal TiZrNi. The colouring scheme is based on an arbitrarily selected direction. The triangle on the right is the domain of that direction. The vector \mathbf{d}_3 is parallel to $\mathbf{a}_1 + \mathbf{a}_5 - \mathbf{a}_6$, i.e. to one of the threefold symmetry axes. The map was not subject to any cleanup. Boundaries with misorientations exceeding 3° are marked in black.

The modified software is universal in the sense that with $n = 3$ it reduces to the original program for indexing data from periodic crystals. It is also applicable to periodic crystals with reflection indices specified in frames with n larger than 3 (Morawiec, 2016). In particular, it can be applied to data specified in a hexagonal four-index setting or in quadray coordinates (Her, 1995; Čomić & Nagy, 2016).

The principles described above apply to diffraction patterns of various types. In particular, they can be used to obtain orientations from patterns generated by EBSD. One only needs to take into account that, with the usual EBSD band detection, the magnitudes of the scattering vectors are not available. This just means that the vectors of both G and H are normalized to 1.

3. Example

The performance of the program is illustrated on polycrystalline EBSD data. The data for suction-cast icosahedral TiZrNi are the same as those used by Winkelmann *et al.* (2020) and Cios *et al.* (2020). Diffraction patterns were collected using *OIM* software (EDAX-AMETEX Inc., USA). The software detects bands in the patterns by Hough transformation and saves (Duda–Hart) line parameters corresponding to the bands (Duda & Hart, 1972). These parameters were converted to normalized scattering vectors; for each line, its position was used to get the coordinates s_i^L of the unit vector perpendicular to the plane containing the line and the point of origin of the pattern. Sets of the coordinates s_i^L constitute the input of *KiKoCh2*. The frame (6) with $a = 1$ was used. For the

material under consideration, the strongest reflections belong to two families; the scattering vectors of the first family are along fivefold axes, and the vectors of the second one are along twofold axes. Therefore, the indices of representatives of the families were specified as $l_1l_2l_3l_4l_5l_6 = 100000$ and 110000 , respectively; see Bancel *et al.* (1985). The input file also contained the 60 proper symmetry operations of the icosahedron.

The file was processed by the modified *KiKoCh2*. For almost all diffraction patterns, the number of detected bands was eight. Of the $799 \times 625 = 499\,375$ patterns, ten patterns were not solved; in all these cases, the number of detected bands was smaller than three. With *KiKoCh2*, the quality of an individual solution is quantitatively characterized by the number N_u of indexed bands and the fit q of the detected and theoretical scattering vectors.¹ N_u and q depend on the tolerances used for matching the vectors, but with the default tolerances of *KiKoCh2* the average number of indexed bands was 7.66 and the average fit was 0.78° . The rate of indexing (serial computation on a 2.6 GHz PC) was more than 2.6×10^4 patterns per second.

An additional small program for displaying the orientation map was written. The resulting map is shown in Fig. 2. It is similar to those obtained by Winkelmann *et al.* (2020) and Cios *et al.* (2020).

¹ The fit is the arccosine of the average dot product of the detected and matching theoretical vectors. The dot product of an individual pair of vectors is $\delta^{ij}s_i^L \cdot O_j^k s_k^L = \cos \alpha$, where α is the angle between the vectors. With N_u pairs, one has $q = \arccos(\sum_{i=1}^{N_u} \cos \alpha_i / N_u) \simeq (\sum_{i=1}^{N_u} \alpha_i^2 / N_u)^{1/2}$, i.e. the fit is close to the root mean square of the angles α_i .

Table 1

Values of $\tau L_i - \xi_i$ for ξ_i listed in the text and integer L_i with absolute values not exceeding 4.

For each i , the numbers $\tau L_i - \xi_i$ closest to integers are marked in bold.

L_1	-4	-3	-2	-1	0	1	2	3	4
$\tau L_1 - \xi_1$	-7.46	-5.84	-4.22	-2.61	-0.99	0.63	2.25	3.87	5.48
L_2	-4	-3	-2	-1	0	1	2	3	4
$\tau L_2 - \xi_2$	-7.49	-5.87	-4.25	-2.64	-1.02	0.60	2.22	3.84	5.45
L_3	-4	-3	-2	-1	0	1	2	3	4
$\tau L_3 - \xi_3$	-6.49	-4.87	-3.25	-1.64	-0.02	1.60	3.22	4.84	6.46

4. Final remarks

Automatic determination of crystallite orientations by indexing detected diffraction reflections is a fast and convenient tool for creating orientation maps of polycrystalline materials. However, it has not been previously available for quasicrystals. This paper has described modifications to software designed for periodic crystals that allow it to be used for quasicrystals.

The described modifications were implemented in the existing program *KiKoCh2*. The modified version of *KiKoCh2* for Windows can be downloaded from <http://imim.pl/personal/adam.morawiec/>. The package also contains a short set of instructions for the program and example data files. For illustration, *KiKoCh2* was applied to the indexing of EBSD bands detected using a commercial EBSD system. A clear orientation map of suction-cast TiZrNi icosahedral quasicrystal was constructed.

As has been the case with periodic crystals, the implementation of quasicrystal orientation determination in automatic orientation mapping systems will open other possibilities such as crystallographic texture determination, phase discrimination, determination of orientation relationships *etc.*

APPENDIX A

Indices of computed scattering vector in frame (6)

Below is a procedure for determining reflection indices in the frame (6) for an icosahedral quasicrystal from approximate components of the scattering vector given in the Cartesian system attached to the crystal. Given the approximate coordinates $s_i = \mathbf{s} \cdot \mathbf{e}_i$, the task is to determine the indices l_μ such that $l_\mu \mathbf{a}^\mu \simeq \mathbf{s} = s_i \mathbf{e}^i$. The indices l_μ satisfy the relationship

$$A_\mu^i s_i = (\mathbf{a}_\mu \cdot \mathbf{e}^i) s_i = \mathbf{a}_\mu \cdot \mathbf{s} \simeq \mathbf{a}_\mu \cdot (l_\nu \mathbf{a}^\nu) = (\mathbf{a}_\mu \cdot \mathbf{a}^\nu) l_\nu = g_\mu^\nu l_\nu, \quad (7)$$

where $g_\mu^\nu = \mathbf{a}_\mu \cdot \mathbf{a}^\nu$ are entries of a projection matrix. With the frame (6) and its dual \mathbf{a}_μ , the explicit form of $g_\mu^\nu l_\nu \simeq A_\mu^i s_i$ is

$$\begin{aligned} \sqrt{5}l_1 - l_2 + l_3 + l_4 + l_5 - l_6 &\simeq a(s_1/\tau + s_2) \\ -l_1 + \sqrt{5}l_2 - l_3 - l_4 + l_5 - l_6 &\simeq a(s_1/\tau - s_2) \\ l_1 - l_2 + \sqrt{5}l_3 - l_4 + l_5 + l_6 &\simeq a(s_2/\tau + s_3) \\ l_1 - l_2 - l_3 + \sqrt{5}l_4 - l_5 - l_6 &\simeq a(s_2/\tau - s_3) \\ l_1 + l_2 + l_3 - l_4 + \sqrt{5}l_5 - l_6 &\simeq a(s_3/\tau + s_1) \\ -l_1 - l_2 + l_3 - l_4 - l_5 + \sqrt{5}l_6 &\simeq a(s_3/\tau - s_1). \end{aligned} \quad (8)$$

This system of approximate equations can be solved with respect to integer l_μ in various ways. One simple approach is to take the solutions of the first, third and fifth equations with respect to l_2, l_4 and l_6 which are

$$\begin{aligned} l_2 &\simeq l_5 + \tau(l_1 + l_3) - \xi_1 \\ l_4 &\simeq l_1 + \tau(l_3 + l_5) - \xi_2 \\ l_6 &\simeq l_3 + \tau(l_5 + l_1) - \xi_3 \end{aligned} \quad (9)$$

or

$$K_i \simeq \tau L_i - \xi_i, \quad (10)$$

where $i = 1, 2, 3$,

$$\begin{aligned} K_1 &= l_2 - l_5 & L_1 &= l_1 + l_3 \\ K_2 &= l_4 - l_1 & L_2 &= l_3 + l_5 \\ K_3 &= l_6 - l_3 & L_3 &= l_5 + l_1 \end{aligned} \quad (11)$$

and

$$\begin{aligned} \xi_1 &= a(s_1/\tau + \tau s_2 + s_3)/2 \\ \xi_2 &= a(s_2/\tau + \tau s_3 + s_1)/2 \\ \xi_3 &= a(s_3/\tau + \tau s_1 + s_2)/2. \end{aligned} \quad (12)$$

Knowing the coordinates s_j ($j = 1, 2, 3$), one determines ξ_i . The next step is to obtain the integers K_i and L_i satisfying the approximate relationship (10). This can be done by computing $\tau L_i - \xi_i$ for all L_i with small absolute values $|L_i| \leq L_{\text{limit}}$, and by choosing the pairs of L_i and $K_i = \lfloor \tau L_i - \xi_i \rfloor$ for which $\tau L_i - \xi_i$ is closest to an integer. Knowing K_i and L_i , one obtains the indices l_μ by solving equations (11) or explicitly from

$$\begin{aligned} l_1 &= (L_1 - L_2 + L_3)/2 & l_2 &= l_5 + K_1 \\ l_3 &= (L_2 - L_3 + L_1)/2 & \text{and } l_4 &= l_1 + K_2 \\ l_5 &= (L_3 - L_1 + L_2)/2 & l_6 &= l_3 + K_3. \end{aligned} \quad (13)$$

The procedure works only if the errors on s_i and L_{limit} are sufficiently small. Therefore, in general, additional filters for rejecting unexpected sets of indices are needed.

It is worth illustrating the above scheme with a worked example. Let $a = 1$, and let the Cartesian components of the vector \mathbf{s} be $s_1 \simeq -0.96$, $s_2 \simeq 0.58$ and $s_3 \simeq 1.63$. With these

numbers, equations (12) lead to $\xi_1 \simeq 0.9876$, $\xi_2 \simeq 1.018$ and $\xi_3 \simeq 0.01704$. The values of $\tau L_i - \xi_i$ for integer L_i such that $|L_i| \leq L_{\text{limit}} = 4$ are listed in Table 1. Based on this table, one has $K_1 = \lfloor -0.99 \rfloor = -1$ and $L_1 = 0$, $K_2 = \lfloor -1.02 \rfloor = -1$ and $L_2 = 0$, $K_3 = \lfloor -0.02 \rfloor = 0$ and $L_3 = 0$. By using equations (13), one obtains the indices corresponding to \mathbf{s} , which are $l_1 l_2 l_3 l_4 l_5 l_6 = 0\bar{1}0\bar{1}00$.

Acknowledgements

I am very grateful to Grzegorz Cios for providing me with the file with positions of EBSD bands, and to Stuart Wright for clarifying some details about this file.

References

- Baker, A., Caputo, M., Hampikian, H., Simpson, L. & Li, C. (2017). *Mater. Sci. Appl.* **8**, 509–520.
- Bancel, P. A., Heiney, P. A., Stephens, P. W., Goldman, A. I. & Horn, P. M. (1985). *Phys. Rev. Lett.* **54**, 2422–2425.
- Becker, H. & Leineweber, A. (2018). *Mater. Charact.* **141**, 406–411.
- Ben-Israel, A. & Greville, T. N. E. (2003). *Generalized Inverses, Theory and Applications*. New York: Springer.
- Cahn, J. W., Shechtman, D. & Gratias, D. (1986). *J. Mater. Res.* **1**, 13–26.
- Cios, G., Nolze, G., Winkelmann, A., Tokarski, T., Hielscher, R., Strzałka, R., Bugański, I., Wolny, J. & Bała, P. (2020). *Ultramicroscopy*, **218**, 113093.
- Čomić, L. & Nagy, B. (2016). *Acta Cryst.* **A72**, 570–581.
- Duda, R. O. & Hart, P. E. (1972). *Commun. ACM*, **15**, 11–15.
- Elser, V. (1985). *Phys. Rev. B*, **32**, 4892–4898.
- Her, I. (1995). *Acta Cryst.* **A51**, 659–662.
- Katz, A. & Duneau, M. (1986). *J. Phys. Fr.* **47**, 181–196.
- Labib, F., Ohhashi, S. & Tsai, A. P. (2019). *Philos. Mag.* **99**, 1528–1550.
- Labib, F., Okuyama, D., Fujita, N., Yamada, T., Ohhashi, S., Morikawa, D., Tsuda, K., Sato, T. J. & Tsai, A. P. (2020). *J. Phys. Condens. Matter*, **32**, 485801.
- Leskovar, B., Šturm, S., Samardžija, Z., Ambrožič, B., Markoli, B. & Naglič, I. (2018). *Scr. Mater.* **150**, 92–95.
- Morawiec, A. (2016). *Acta Cryst.* **A72**, 548–556.
- Morawiec, A. (2020). *Acta Cryst.* **A76**, 719–734.
- Morawiec, A. (2022). *Indexing of Crystal Diffraction Patterns. From Crystallography Basics to Methods of Automatic Indexing*. Cham: Springer.
- Singh, S., Lenthe, W. C. & De Graef, M. (2019). *Philos. Mag.* **99**, 1732–1750.
- Tanaka, R., Ohhashi, S., Fujita, N., Demura, M., Yamamoto, A., Kato, A. & Tsai, A. P. (2016). *Acta Mater.* **119**, 193–202.
- Winkelmann, A., Cios, G., Tokarski, T., Nolze, G., Hielscher, R. & Koziel, T. (2020). *Acta Mater.* **188**, 376–385.